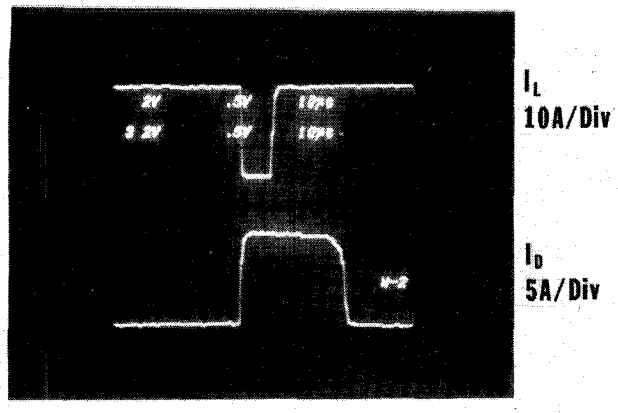

Fig. 5. Laser current pulse versus ON time of a p-i-n diode.

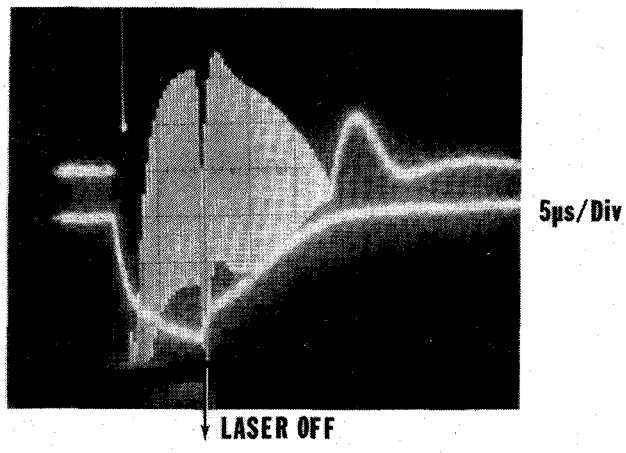

Fig. 6. HF signal after passing through the switch at 400 V bias voltage.

Thus, we have limited our measurements to a window of 10 μs pulse width and 1 Hz repetition rate.

As the laser power increases, more electron–hole pairs are created in the i region of the p-i-n diode and the resistance, and hence the insertion loss, drop. Table I illustrates this effect and shows that at an incident laser power of 116.7 W the insertion loss is still dropping. At the time of these measurements, 116.7 W was the maximum available power. Table II depicts the change (increase) in insertion loss with bias voltage. To minimize the insertion loss at higher voltages (which are needed as the RF power requirement is increased), the 50 Ω bias resistor (see Fig. 4) should be increased proportionately. Isolation (switch off, no light) decreases with frequency (Table III); in the OFF state the p-i-n diode is similar to a fixed capacitor.

It is important to note at this point that many applications require CW switching. The HF antenna coupler is one important application (an antenna coupler is a tunable matching circuit between a high-Q antenna and a generator across a very wide band). For this application, we have chosen to use a silicon p-i-n diode in order to take advantage of the long carrier lifetime.

Fig. 5 depicts the laser current pulse of 10 μs (top) versus the p-i-n diode's ON time. This ON time is more than three times the duration of the laser pulse. We have utilized this concept by using pulse 2-D laser arrays having an optical power output of 116 W to close a switch for a duration of about twice that of the laser pulse itself. This technique is very important in reducing the complexity of the antenna coupler system, and in realizing a CW switch with a pulsed laser array. It is conceivable to increase this ratio, which is a function of the carrier lifetime and the voltage applied. Fig. 6 depicts the ON state of a p-i-n switch, lower trace (the OFF point of the laser is indicated), and the HF signal propagating through the switch at 400 V bias voltage. The laser diode is on for 10 μs, while the switch (p-i-n device) is on for an additional 15–20 μs.

III. Conclusion

We have demonstrated, for the first time, the feasibility of a laser-activated semiconductor switch at low frequencies (2–30 MHz) with an RF power capability of up to 250 W. This approach, when fully developed, will have the following advantages: small size, jitter-free switching, fast rise time, noise immunity, and high voltage isolation, in addition to having a CW switch by utilizing pulsed laser.

Acknowledgment

The authors sincerely appreciate the support of R. Bartolini and M. Ettenberg.

References

[1] R. N. Hall, "Power rectifiers and transistors," *Proc. IRE*, vol. 40, pp. 1512–1518, Nov. 1952.
[2] M. B. Prince, "Diffused p-n junction silicon rectifiers," *Bell Syst. Tech. J.*, vol. 35, pp. 661–684, May 1956.
[3] G. Lucovsky, M. F. Lasser, and R. B. Emmons, "Coherent Light Detection Utilizing Solid State Photodiodes," in *Electrochem. Soc. Spring Meeting: Electron. Division Abstracts*, vol. 11, no. 1, pp. 284–285, May 1962.
[4] R. P. Riesz, "High speed photodiodes," *Rev. Sci. Instr.*, pp. 994–998, Sept. 1962.
[5] L. L. Anderson, "The PIN junction photodiodes as a detector of light modulated at microwave frequencies," in *1963 Int. Solid-State Circuits Conf. Dig.*, Feb. 1963, pp. 114–115.
[6] D. H. Auston, "Picosecond optoelectronic switching and gating in silicon," *Appl. Phys. Lett.*, vol. 26, no. 3, Feb. 1, 1975.
[7] P. LeFur and D. H. Auston, "A kilovolt picosecond optoelectronic switch and Pockel's cell," *Appl. Phys. Lett.*, vol. 28, no. 1, Jan. 1, 1976.
[8] C. Lee, "Picosecond optoelectronic switching in GaAs," *Appl. Phys. Lett.*, vol. 30, no. 2, Jan. 15, 1977.
[9] W. C. Nunnally and R. B. Hammond, "80-MW photoconductor power switch," *Appl. Phys. Lett.*, vol. 44, no. 10, May 15, 1984.
[10] A. Rosen, R. U. Martinelli, A. Schwarzmann, G. J. Brucker, and G. A. Swartz, "High-power low-loss PIN diodes for phased array radar," *RCA Rev.*, vol. 39, pp. 22–58, Mar. 1979.
[11] A. Rosen *et al.*, "Optically activated p-i-n diode switch utilizing a two-dimensional laser array at 808 nm as an optical source," *IEEE Trans. Electron Devices*, vol. 36, pp. 367–374, Feb. 1989.
[12] M. Caulton, A. Rosen, P. J. Stabile, and A. Gombar, "p-i-n diodes for low-frequency high-power switching applications," *IEEE Trans. Microwave Theory Tech.*, vol. MTT-30, pp. 875–881, June 1982.
[13] A. S. Daryoush *et al.*, "Optically controlled three terminal microwave PIN diode and its application," in *Proc. 1985 SBMO Int. Microwave Symp.* (Campinas, Brazil), pp. 298–302.

Analysis of Rectangular Spiral Transformers for MMIC Applications

ANDRE BOULOUARD, MEMBER, IEEE,
AND MICHEL LE ROUZIC

***Abstract*—To evaluate rectangular spiral transformers for use in microwave monolithic integrated circuits (MMIC's) on GaAs substrate, we have calculated the chain matrices of multiconductor coupled line sections**

Manuscript received February 17, 1988; revised March 10, 1989.
The authors are with the Centre National d'Etudes des Telecommunications, CNET/LAB/MER/MLS, Lannion B, 22301 France.
IEEE Log Number 8928330.

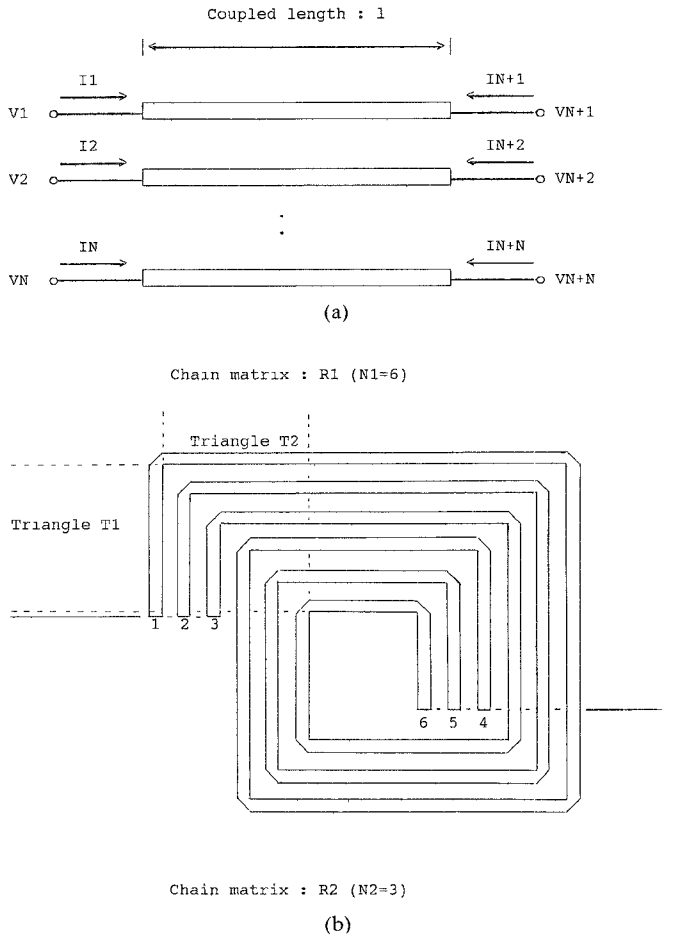

Fig. 1 Schematic of a 1.5 turn rectangular spiral triformer. (a) Multiconductor coupled line section (b) Triformer layout

and bends from multimode characteristic impedances and effective dielectric constants. A new kind of MMIC transformer, called a triformer, has been analyzed by this method and may be used as an integrated circuit balun. Theoretical results are presented for components over the range 1–10 GHz and compared to measurements.

I. Introduction

Rectangular spiral transformers that operate in the gigahertz frequency range have been reported elsewhere as useful coupling and matching elements [1], [2]. As shown in Fig. 1, the layout of a typical transformer consists of a series of turns of thin metallized coupled microstrip lines. The theoretical approach used in [3] for predicting the electrical behavior of planar spiral transformers is applied here with the following simplifying assumptions:

i) the capacitive and negative mutual coupling between opposite and adjacent spiral sides is neglected;
ii) spiral corners are modeled by single 90° bends;
iii) the parasitic effect of the lead-out bridge connecting the center of the spiral to the outer circuitry is ignored.

As was pointed out in [4], these secondary effects should be taken into account for accurate prediction of the electrical behavior of the transformer up to and beyond the first resonance frequency. The effect of the lead-out bridge may be accounted for by Y to chain matrix conversion, as indicated in [5].

Nevertheless, the analysis method adopted here is quite general in nature and gives results accurate enough to be useful.

II. Method of Analysis

In this approach, the multiconductor structure is broken down into a series of parallel coupled line and coupled bend substructures. Using this method, each substructure chain matrix is calculated separately and cascaded with the preceding one to obtain the chain matrix of the complete structure [6].

A. Multiconductor Coupled Line Section Chain Matrix

The theory of wave propagation on multiconductor transmission lines with inhomogeneous dielectrics presented in [7] is applied to a section of N coupled lines of equal length l (cf. Fig. 1) to obtain the multidimensional $(2N,2N)$ chain matrix R defined as follows:

$$\begin{vmatrix} V1 \\ I1 \\ V2 \\ I2 \\ \vdots \\ VN \\ IN \end{vmatrix} = R \cdot \begin{vmatrix} VN+1 \\ IN+1 \\ VN+2 \\ IN+2 \\ \vdots \\ VN+N \\ IN+N \end{vmatrix} \tag{1}$$

where Vk and Ik are the voltage and current at port $k=1,\cdots,N+N$:

$$R(2m-1,2n-1) = A(m,n) \qquad (m,n=1\cdots N) \tag{2}$$

$$R(2m-1,2n) = B(m,n) \tag{3}$$

$$R(2m,2n-1) = C(m,n) \tag{4}$$

$$R(2m,2n) = D(m,n) \tag{5}$$

where

$$A = Mv \cdot \cosh(\Gamma \cdot l) \cdot Mv^{-1} \tag{6}$$

$$B = Mv \cdot \sinh(\Gamma \cdot l) \cdot Mv^{-1} \cdot Z0 \tag{7}$$

$$C = Mi \cdot \sinh(\Gamma \cdot l) \cdot Mi^{-1} \cdot Y0 \tag{8}$$

$$D = Mi \cdot \cosh(\Gamma \cdot l) \cdot Mi^{-1}. \tag{9}$$

Mv, Mi, $Z0$, $Y0$, $\cosh(\Gamma \cdot l)$, $\sinh(\Gamma \cdot l)$, and Γ are the frequency-dependent (N, N) matrices of multiple coupled strip transmission lines and are obtained from a data base generated with the aid of the program MCLINE [8].

B. Multiconductor Coupled Line Bend Chain Matrix

As shown in Fig. 1, the multiconductor bend substructure is divided into two triangles of N coupled lines and a network of isolated discontinuities. The chain matrix $T1$ of the first triangle is computed from a cascade of coupled line sections as follows:

$$T1 = \begin{vmatrix} & & 0 & 0 \\ & U1 & \vdots & \vdots \\ & & \vdots & \vdots \\ 0 & \cdots & 1 & 0 \\ 0 & \cdots & 0 & 1 \end{vmatrix} \tag{10}$$

where $U1$ is a $(2N-2,2N-2)$ matrix partitioned into $N-1$ submatrices Wi, each of dimensions $(2N-2,2)$:

$$U1 = | WN-1 | WN-2 | \cdots | W2 | W1 |. \tag{11}$$

Each submatrix Wi is calculated from partitions Xi and Yi of the chain matrix Si for a section of $N-i$ coupled lines of length

equal to $W+S$:

$$WN-1 = X1 \cdot X2 \cdots XN-2 \cdot YN-1 \quad (12)$$

$$WN-2 = X1 \cdot X2 \cdots XN-3 \cdot YN-2 \quad (13)$$

$$\vdots$$

$$W2 = X1 \cdot Y2 \quad (14)$$

$$W1 = Y1 \quad (15)$$

$$Si = |\, Xi \mid Yi \,|. \quad (16)$$

Here Xi and Yi are partitions of dimensions $(2N-2i, 2N-2i-2)$ and $(2N-2i, 2)$ respectively.

The chain matrix Tb of the isolated discontinuities is calculated from [9] using a lumped tee network model for a single bend:

$$Rb = \begin{vmatrix} Ab & Bb \\ Cb & Db \end{vmatrix}. \quad (17)$$

Rb is therefore a (2,2) chain matrix.

$$Tb = \begin{vmatrix} Rb & & & \\ & Rb & & 0 \\ & & \ddots & \\ & 0 & & Rb \\ & & & & Rb \end{vmatrix} \quad (18)$$

Tb is therefore a $(2N,2N)$ quasi-diagonal chain matrix.

The chain matrix $T2$ of the second triangle is obtained from $T1$ by the following formula:

$$T2 = E \cdot T1^{-1} \cdot E \quad (19)$$

where E is a $(2N,2N)$ diagonal matrix defined as

$$E = \begin{vmatrix} +1 & & & & \\ & -1 & & & \\ & & \ddots & & \\ & & & +1 & \\ & & & & -1 \end{vmatrix}. \quad (20)$$

The chain matrix T of the complete bend is then calculated by cascading $T1$, Tb, and $T2$:

$$T = T1 \cdot Tb \cdot T2. \quad (21)$$

C. Multiconductor Coupled Line Transformer Chain Matrix

As shown in Fig. 1, the transformer is subdivided into two sections, between ports 1 and 2:

i) an upper-side section characterized by the chain matrix $R1$ of dimensions $(2N1, 2N1)$,
ii) a lower-side section characterized by the chain matrix $R2$ of dimensions $(2N2, 2N2)$

where $N1$ and $N2$ are the numbers of coupled lines in each section.

The chain matrices $R1$ and $R2$ are calculated by cascading sections of coupled lines and bends as stated above. To account for feedback effects, the chain matrix $R1$ is further partitioned as follows:

$$R1 = \left| \begin{array}{c|c} R11 & R12 \\ \hline R21 & R22 \end{array} \right| \quad (22)$$

where $R11$, $R12$, $R21$, and $R22$ are of dimensions $(2N1-2N2, 2N2)$, $(2N1-2N2, 2N1-2N2)$, $(2N2, 2N2)$, and $(2N2, 2N1-2N2)$ respectively.

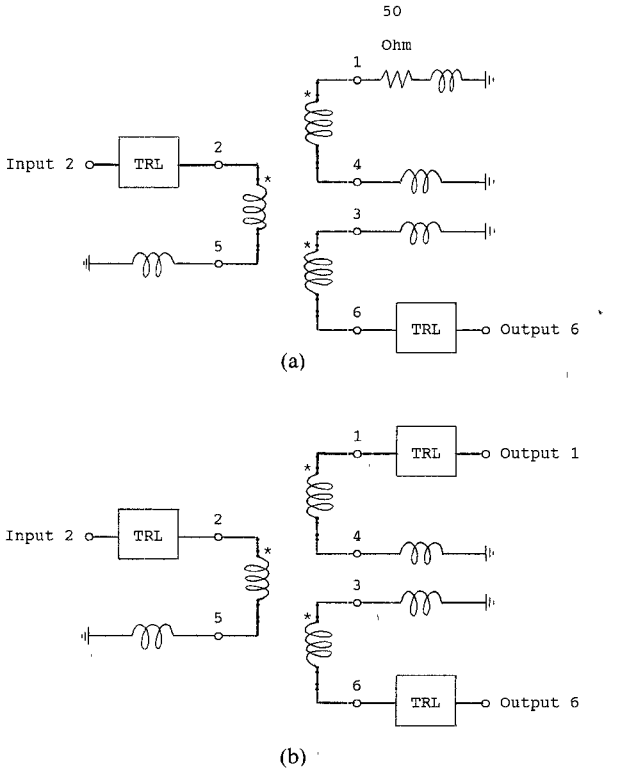

Fig. 2. Electrical models of MMIC triformers. (a) 1 5 turn triformer ($W=5$ μm, $S=5$ μm). (b) 1 turn triformer ($W=10$ μm, $S=5$ μm).

The chain matrix R of the complete transformer is then obtained after some matrix algebra as follows:

$$R = R12 + R11 \cdot (U - R2 \cdot R21)^{-1} \cdot R2 \cdot R22 \quad (23)$$

where U is the $(2N2, 2N2)$ unit matrix.

III. Calculations and Results

A computer program has been developed for the analysis and optimization of planar inductors and transformers and has been used to calculate various MMIC components [10]. A new kind of transformer, which is a planar version of a three-line RUTHROFF transformer [11], is shown in Fig. 1 and is referred to as a triformer.

Using values of epsr = 12.9, tan d = 0.0003, metal thickness = 2 μm, metal resistivity = 0.03 $\Omega \cdot \mu$m, $W=10$ μm and 5 μm, $S=5$ μm, and substrate height $H=100$ μm, the theoretical S parameter values are calculated for the triformers shown in Fig. 2 over the frequency range 1–10 GHz.

The computed S parameters compare favorably with the measured parameters of MMIC triformers shown in Fig. 3. The differential phase shift between output 1 and output 6 remains nearly equal to 182°, as shown in Fig. 4; therefore, this triformer can be considered a wide-band balun

IV. Conclusions

Multidielectric planar structures such as transformers and triformers have been analyzed by cascading multidimensional chain matrices. The distributed-line model facilitates the use of these elements in MMIC applications as wide-band transformers and baluns. High-speed routines suitable for inclusion in CAD packages for desktop PC's have been implemented and used to calculate S parameters.

Wide-band MMIC triformers have been fabricated and measured, showing good agreement between theory and measurement

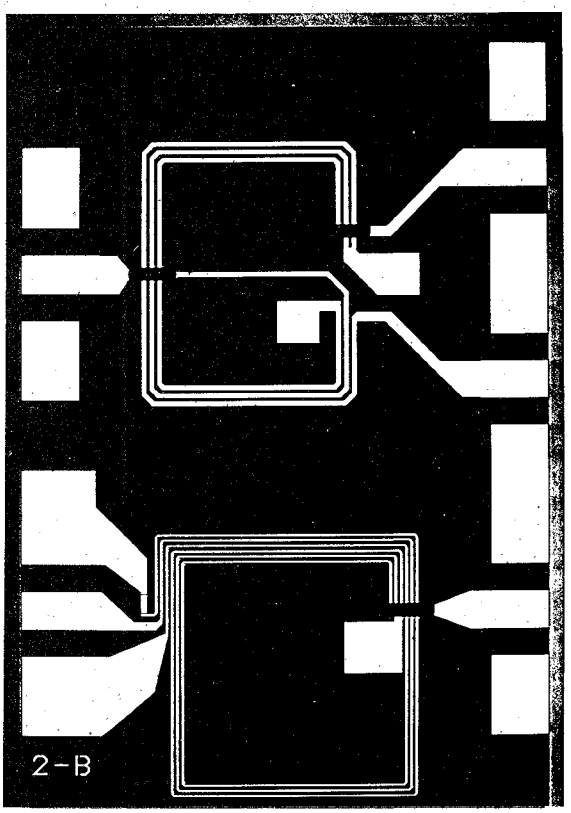

Fig. 3. Photograph of MMIC triformers.

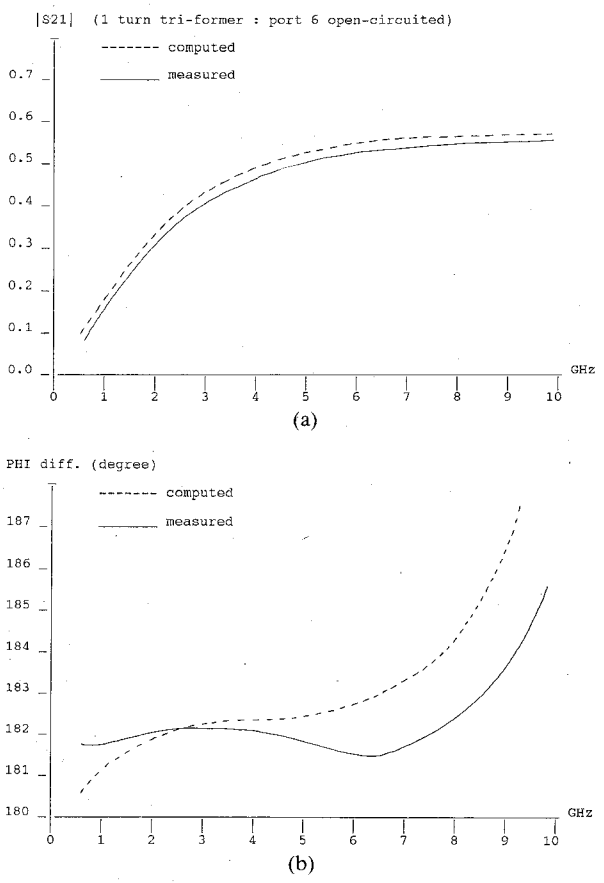

Fig. 4. Comparison of computed and measured S parameters. (a) Magnitude. (b) Differential phase shift.

over the frequency range 1–10 GHz. The application of these devices as wide-band baluns for MMIC balanced mixers is foreseen.

ACKNOWLEDGMENT

The authors would like to thank M. Le Brun and G. Montoriol from the THOMSON/THM/DAG MMIC foundry for providing the necessary assistance and MMIC measurement results.

REFERENCES

[1] D. Ferguson *et al.*, "Transformer coupled high-density circuit technique for MMIC," in *1984 IEEE Microwave and Millimeter-Wave Monolithic Circuits Symp. Dig.*, pp. 34–36.

[2] R. H. Jansen, "LINMIC: A CAD package for the layout-oriented design of single- and multi-layer MICs/MMICs up to mm-wave frequencies," *Microwave J.*, pp. 151–161, Feb. 1986.

[3] L. Wiemer, R. H. Jansen, I. D. Robertson, and J. B. Swift, "Computer simulation and experimental investigation of square spiral transformers for MMIC applications," IEE Collection on CAD of MICs, Dig. No. 1985/99, London, Feb. 1–5, 1985.

[4] R. H. Jansen and L. Wiemer, "Multi-conductor hybrid-mode approach for the design of MIC couplers and lumped elements including loss, dispersion and parasitics," in *Proc. 14th European Microwave Conf.* (Liege, Belgium), 1984, pp. 142–147.

[5] P. R. Sheperd, "Analysis of square-spiral inductors for use in MMIC's," *IEEE Trans. Microwave Theory Tech.*, vol. MTT-34, pp. 467–472, Apr. 1986.

[6] J. Siegl, "PLANAR—ein program zur Simulation von Hochfrequenzschaltungen mit verteilten Leitungsstrukturen," *Frequenz*, vol. 40, no. 8, pp. 209–213, 1986.

[7] K. D. Marx, "Propagation modes, equivalent circuits, and characteristic terminations for multiconductor transmission lines with inhomogeneous dielectrics," *IEEE Trans. Microwave Theory Tech.*, vol. MTT-21, pp. 450–457, July 1973.

[8] R. H. Jansen, "A novel CAD tool and concept compatible with the requirement of multi-layer GaAs MMIC technology," in *1985 IEEE MTT-S Int. Microwave Symp. Dig.* (St. Louis, MO), pp. 711–714.

[9] M. Kirschning and R. H. Jansen, "Measurement and computer-aided modeling of microstrip discontinuities by an improved resonator method," in *1983 IEEE MTT-S Int. Microwave Symp. Dig.*, pp. 495–497.

[10] A. Boulouard, "MICANA: a Microwave cascaded networks Analysis and optimisation desktop computer program," CNET-LANNION-B France, Jan. 1988.

[11] C. L. Ruthroff, "Some broadband transformers," *Proc. IRE*, vol. 47, pp. 1337–1342, Aug. 1959.

Analysis of Edge-Coupled Elliptical (Oval) Rods Between Infinite Ground Planes

KODUKULA V. S. RAO, MEMBER, IEEE, AND PRAKASH BHARTIA, FELLOW, IEEE

***Abstract*—The paper presents an analysis of the even- and odd-mode impedances for a generalized edge-coupled structure consisting of two elliptical (oval) conducting rods. Data on the even- and odd-mode impedances for different special cases of the generalized elliptical (oval) structure are presented. Some special cases of the present formulation are compared with results available in the literature.**

I. INTRODUCTION

The analysis of parallel edge-coupled strips has been presented in the literature by Cohn [1]. Wheeler analyzed the transmission properties of a single round wire between two parallel planes [2].

Manuscript received August 19, 1988; revised February 6, 1989. This work was supported by the Natural Sciences and Engineering Research Council of Canada under Grant A-0001.

K. V. S. Rao is with the Laboratory for Electromagnetics and Microwaves, Department of Electrical Engineering, University of Ottawa, Ottawa, Ont., Canada K1N 6N5.

P. Bhartia is with the Department of National Defence, Ottawa, Ont., Canada K1A 0K2

IEEE Log Number 8928328